Domains of τ Protein and Interactions with Microtubules†

N. Gustke, B. Trinczek, J. Biernat, E.-M. Mandelkow, and E. Mandelkow*

Max-Planck-Unit for Structural Molecular Biology, c/o DESY, Notkestrasse 85, D-22603 Hamburg, Germany

Received November 22, 1993; Revised Manuscript Received May 16, 1994®

ABSTRACT: The role of the neuronal microtuble-associated protein τ has been studied by generating a series of τ constructs differing in one or several of its subdomains: length and composition of the repeat domains, extensions of the repeats in the N- or C-terminal direction, constructs without repeats, assembly vs projection domain, and number of N-terminal inserts. The interaction of the mutant τ proteins with microtubules was judged by several independent methods. (i) Direct binding assays between τ and taxol-stabilized microtubules yield dissociation constants and stoichiometries. (ii) Light scattering and X-ray scattering of assembling microtubule solutions reflect the capacity of τ to promote microtubule nucleation, elongation, and bundling in bulk solution. (iii) Dark field microscopy of assembling microtubules allows one to assess the efficiency of nucleation and bundling separately. The repeat region alone, the N-terminal domains alone, or the C-terminal tail alone binds only weakly to microtubules. However, binding is strongly enhanced by combinations such as the repeat region plus one or both of the flanking regions which could be viewed as "jaws" for τ on the microtubule surface (the proline-rich domain P upstream of the repeats and the "fifth" repeat R′ downstream). Such combinations make τ's binding productive in terms of microtubule assembly and stabilization, while the combination of the flanking regions without repeats binds only unproductively. Efficient nucleation parallels strong binding in most cases, i.e., when a construct binds tightly to microtubules, it also nucleates them efficiently and vice versa. In addition, the proline-rich domain P in combination with the repeats R or the flanking domain R′ causes pronounced bundling. This effect disappears when the N-terminal domains (acidic or basic) are added on, suggesting that the τ isoforms are not "bundling proteins" in the proper sense. In spite of the wide range of binding strength and nucleation efficiency, the stoichiometries of binding are rather reproducible (around 0.5 τ/tubulin dimer); this is in remarkable contrast to the effect of certain types of phosphorylation which can strongly reduce the stoichiometry.

(*a*) *MAPs and Microtubule Assembly.* Microtubule-associated proteins (MAPs)[1] derive their name from the fact that they copolymerize with microtubules through cycles of assembly and disassembly. This means that they bind to microtubules. More importantly, however, they also stimulate microtubule assembly and stabilize them, once formed. The tissue- and development-specific stabilization of microtubules is presumably one of the important functions of MAPs [for recent reviews, see Wiche et al. (1991), Chapin and Bulinski (1992), and Lee (1993)]. A number of MAPs have now been cloned and sequenced. Depending on sequence homology, they can be subdivided into several families. The best known family is that of the τ-MAP2-MAP4 proteins [for τ, see Drubin et al. (1984), Lee et al. (1988), and Himmler et al. (1989); for MAP2, Lewis et al. (1988) and Kindler et al. (1990); for MAP4, Aizawa et al. (1990), West et al. (1991), and Chapin and Bulinski (1991)]. They derive from different genes but share several homologous ≈31-residue repeats near their C-termini that are involved in microtubule binding. MAP2 and τ occur in the brain; MAP4 is ubiquitous.

The functions of MAPs are regulated on at least two levels. One is alternative splicing which yields several protein products, and the second is phosphorylation. In the case of τ, human central nervous tissue contains six isoforms with lengths between 352 and 441 residues; they differ by having either three or four repeats in the C-terminal half and zero, one or two inserts near the N-terminus (Goedert et al., 1989). The 3-repeat forms occur preferentially in the fetal stage. Phosphorylation appears to modulate the affinity for microtubules. How this is achieved in vivo is still poorly understood, despite a large number of studies [the complexity was demonstrated for the case of MAP2 by Brugg and Matus (1991)]. Many kinases phosphorylate MAPs, often at multiple sites, but the effect on microtubule binding tends to be only moderate [one exception being the phosphorylation of Ser262 of τ protein; see Biernat et al. (1993)]. In fact, the kinases that phosphorylate brain MAPs most efficiently (such as MAP kinase, GSK-3, or cdk5 in the case of τ; Drewes et al., 1992; Mandelkow et al., 1992; Baumann et al., 1993) are not necessarily the ones that have a strong influence on microtubule stability.

τ protein was one of the first MAPs discovered, characterized biochemically, and cloned (Weingarten et al., 1974; Cleveland et al., 1977; Drubin et al., 1984; Lee et al., 1988; Himmler et al., 1989). The interest in this protein was greatly enhanced by the findings that τ is the main component of the paired helical filaments of Alzheimer's disease and that this pathological τ is abnormally phosphorylated [Grundke-Iqbal et al., 1986; Wood et al., 1986; Wischik et al., 1988; Ishiguro et al., 1991; Bramblett et al., 1993; for review, see Lee and Trojanowski (1992)]. In previous studies, we have shown that certain types of phosphorylation induce an antibody

† This project was supported by the Bundesministerium für Forschung und Technologie and the Deutsche Forschungsgemeinschaft.

* Corresponding author. Tel: (+49) (40) 8998-2810. Fax: (+49) (40) 891314.

® Abstract published in *Advance ACS Abstracts,* July 15, 1994.

[1] Abbreviations: The six isoforms of τ in the human central nervous system are denoted either by the clone names [see Goedert et al. (1989)] or by the numbers of N-terminal inserts (0–2) and repeats (3 or 4). htau23 = ON/3R (352 residues); htau24 = ON/4R (383); htau37 = 1N/3R (381); htau34 = 1N/4R (412); htau39 = 2N/3R (410); htau40 = 2N/4R (441). This sequence coincides with the sequence of ascending M_r on SDS gels [M_r = 48–67 kDa; see Goedert and Jakes (1990)]. MAPs = microtubule-associated proteins; OD = optical density.

0006-2960/94/0433-9511$04.50/0

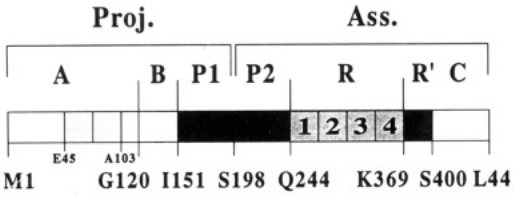

FIGURE 1: Bar diagram of τ protein, isoform htau40 (2N/4R, 441 residues). The two 29-mer inserts (starting at E45) are lightly shaded, and the four repeats are numbered 1–4 (Q244-N368, medium shade). Definition of domains: projection domain, M1-Y197; assembly domain, S198-L441 (separable by chymotryptic cleavage); N-terminal domains A (acidic), M1-G120, B (basic), G120-I151, and P (proline-rich and basic), I151-Q244, separated into P1 and P2 at Y197; repeats R1-R4, Q244-N368, "fifth" repeat R′, K369-S400; and C = C-terminal tail, G401-L441. The alignment of the repeats is shown below; in this convention, R2 coincides with the sequence coded by exon 10 (Goedert et al., 1989; Andreadis et al., 1992). Each repeat consists of a region of high homology (the repeats proper, underlined) and a less homologous "linker" region. The sequence of R′ shows only the low homology aspect and thus is usually not considered a repeat in itself [but see Chapin and Bulinski (1992)].

```
R1: 244 QTAPVPMPDLKN-VKSKIGSTENLKHQPGGGK  274

R2: 275 VQIINKKLDLSN-VQSKCGSKDNIKHVPGGGS  305

R3: 306 VQIVYKPVDLSK-VTSKCGSLGNIHHKPGGGQ  336

R4: 337 VEVKSEKLDFKDRVQSKIGSLDNITHVPGGGN  368

R': 369 KKIETHKLTFRENAKAKTDHG-AEIVYKSPVVS 400
```

reactivity similar to that of Alzheimer paired helical filaments (Lichtenberg et al., 1992; Biernat et al., 1992) and that the repeat domain of τ can self-assemble into PHF-like filaments in vitro (Wille et al., 1992).

In this paper, we have asked how the different domains of τ affect the interactions with microtubules. Our approach was to synthesize a variety of τ constructs differing in their composition of domains and then to probe their interactions with microtubules by several independent methods, yielding separate information on binding constants and stoichiometries, induction of assembly, and microtubule bundle formation. As discussed later, our studies are complementary to the anlaysis of MAP domains by other authors, notably those on MAP2, MAP4, and τ (Lee et al., 1989; Ennulat et al., 1989; Joly & Purich, 1990; Butner & Kirschner, 1991; Aizawa et al., 1991; Lee & Rook, 1992; Kanai et al., 1992; Brandt & Lee, 1993; Chen et al., 1992; Goode & Feinstein, 1994).

(*b*) *Domains of τ Protein.* As an introduction to the results, it is useful to consider different ways of defining protein domains and how they might affect microtubule behavior. Figure 1 shows the sequence of τ; Table 1 contains diagrams of the constructs used in this study. The most pertinent definition of a domain is that of a folding unit since these usually correspond to functional units (Schulz & Schirmer, 1979). This criterium is not testable here since the 3D-structure of τ is unknown. A second definition is based on limited proteolysis; the rationale for this is that the sites most accessible to proteases are often located in loops connecting different folding units. In the case of τ, limited chymotryptic cleavage at Tyr197 separates the N-terminal domain (residues 1–197 in the numbering of the isoform htau40, Figure 1) and the C-terminal domain (residues 198–441; Steiner et al., 1990). Thirdly, domains could be defined in terms of different interactions with other molecules. For example, the C-terminal chymotryptic fragment binds to microtubules while the N-terminal one does not, leading to the notion of "assembly" and "projection" domains, in analogy with MAP2 (Vallee & Borisy, 1977).

A fourth definition of domains can be based on the character of the primary sequence. The N-terminal third of τ (residues 1 to ≈150, Figure 1) is highly charged; it can be subdivided into the acidic domain A (1–120) and the more basic domain B (120–150). The following region 150–240 is also basic, but the more prominent feature is that this domain is rich in prolines. We refer to it as the P domain (subdivided into P1 and P2 at Tyr197). The region 244–368 is characterized by three or four imperfect repeats of 31 or 32 residues; they were recognized early on to be involved in microtubule binding (Lee et al., 1988; Himmler et al., 1989). A number of studies have shown that peptides related to this region bind to microtubules, albeit weakly (Joly & Purich, 1990; Ennulat et al., 1989; Butner & Kirschner, 1991; Lee et al., 1989). The region following the repeats (369–441) is often regarded simply as the C-terminal tail. However, since residues 369–400 are weakly homologous to the repeats, we refer to it as R′ (a "fifth" repeat), reserving the term "C" for the terminal residues (400–441). The boundary between domains R′ and C coincides roughly with the secondary chymotryptic cleavage site at Tyr394 (note that MAP4 contains yet another weakly homologous repeat lying between R1 and R2 of τ; Chapin & Bulinski, 1992).

Finally, one could define domains on the basis of the intron–exon structure of the τ gene, especially since the isoforms are generated by alternative splicing (Himmler et al., 1989; Goedert et al., 1989; Andreadis et al., 1992). There are two near N-terminal 29-mer inserts (N1, 45–73, and N2, 74–102, exons 2 and 3) which may be present or absent from domain A but have no noticeable effect in our experiments to be described below. The end of exon 4 (Gln124) nearly coincides with the A/B boundary, exon 7 starts roughly at the beginning of the P domain (Gly144), the second repeat R2 coincides with exon 10, and exons 11 and 12 terminate roughly with the ends of repeats R3 and R4 (at Gly333 and Lys370, respectively). Thus the exon structure shows certain similarities with the domains defined on the basis of protein character.

When considering the relationship between τ and microtubules, it is important to distinguish between different effects. Microtubules must be nucleated, they can then grow or shrink, they can show dynamic instability or be stabilized by different cofactors or proteins, they can bind other proteins, and they can form bundles. τ is best known for binding to microtubules and promoting nucleation and growth in vitro (Cleveland et al., 1977); it stabilizes microtubules after microinjection into fibroblasts (Drubin & Kirschner, 1986), and it even allows the formation of microtubule bundles after transfection (Kanai et al., 1989, 1992; Knops et al., 1991). These effects could be caused by different domains and are not necessarily related to one another. In addition, one should consider the possibility that the function of τ in axons goes beyond the stabilization of microtubules. For example, the N-terminal domains of MAPs could regulate the spacing between microtubules and other cytoskeletal elements (including neighboring microtubules; Chen et al., 1992); they could provide an anchor for enzymes (such as protein kinase A in the case of MAP2; Obar et al., 1989). MAPs occur not only bound to microtubules but also in soluble form. τ can detach from microtubules and aggregate into the paired helical filaments of Alzheimer's disease (Grundke-Iqbal et al., 1986; Bramblett et al., 1993), but this pathological condition could well highlight a state of the protein that is of some other yet unknown physiological relevance.

These examples illustrate that one needs to assay the τ–microtubule interactions by assays sensitive to different effects. We have employed mainly three methods. One is

Table 1: Constructs of τ Protein and Parameters of Microtubule Binding and Assembly[a]

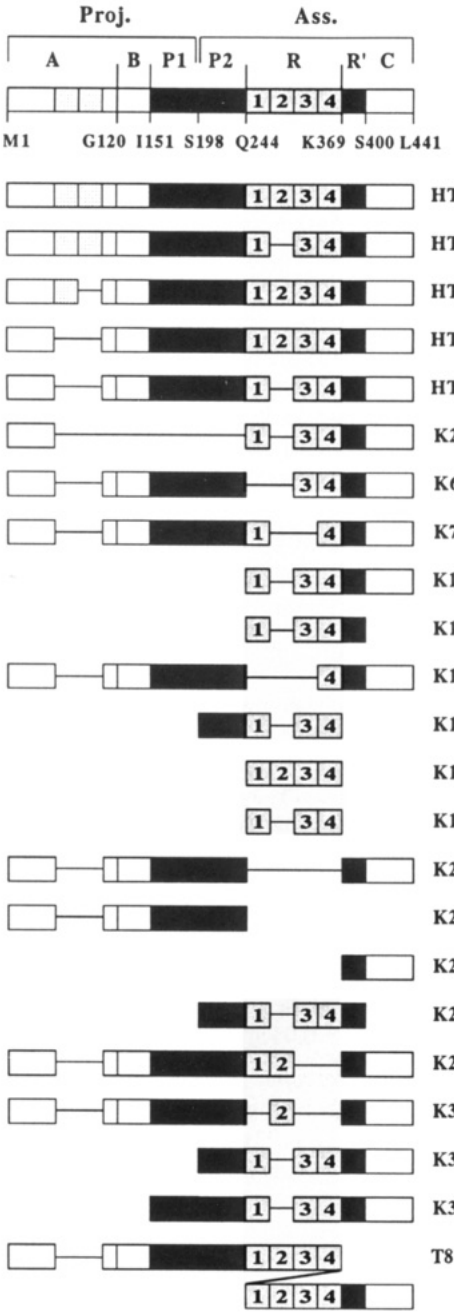

	Kd [μM]	Stoi.-metry n	lag-time [s]	ini.-rate [OD/min]	OD max 350 nm	nuclea-tion	bund-ling
HT40	1.1	0.46	5	0.92	0.16	+++	no
HT39	2.9	0.48	14	1.10	0.16	n.d.	n.d.
HT34	1.4	0.43	4	0.72	0.15	n.d.	n.d.
HT24	n.d.	n.d.	5	1.57	0.16	+++	no
HT23	2.5	0.49	10	0.99	0.17	++	no
K2	16.2	0.28	n.d.	n.d.	n.d.	n.d.	n.d.
K6	3.1	0.51	11	1.25	0.17	++	no
K7	2.4	0.46	10	1.33	0.19	++	no
K10	18.5	0.42	29	0.10	0.12	+	no
K12	7.1	0.45	20	0.20	0.17	+	no
K13	4.2	0.45	9	0.78	0.14	+	no
K17	5.3	0.56	14	0.63	0.46	+	yes
K18	25.5	0.51	22	0.04	0.12	+	no
K19	50.9	0.52	40	0.06	0.13	+	no
K23	6.5	0.53	27	0.09	0.12	+	no
K25	$\geq 10^3$	≥0.46	42	0.02	0.08	+	no
K26	$\geq 10^3$	≤0.10	n.d.	n.d.	n.d.	+	no
K27	3.4	0.55	6	1.65	0.30	++	yes
K29	1.2	0.44	6	1.14	0.17	++	no
K30	2.7	0.41	9	1.55	0.17	++	no
K33	1.5	0.52	10	0.38	0.16	++	no
K35	1.0	0.48	6	1.66	0.56	++	yes
T8R2	0.05/10.1	0.3/0.27	9	1.19	0.43	+++	yes
						+ ≤ 50	++ 100-400	+++ ≥400 MT

[a] The constructs on the left are subdivided and shaded as the full τ protein (see Figure 1, and repeated in the table). Dark and medium shaded domains contribute to interaction with microtubules. The dissociation constant K_d (μM) and the stoichiometry n(τ/tubulin dimer at saturation) were derived from the binding curves (see Figure 2). The lag time (s), initial rate of turbidity increase (OD/min), and maximum turbidity after assembly (OD_{max} at 350 nm) were derived from the light scattering traces (see Figure 3). The entries for the efficiency of nucleation and bundling were obtained by video and electron microscopy (see Figures 4 and 5). Symbols for nucleation: +, weak (below 50 microtubules/field); ++, medium (50–400 microtubules/field); +++, strong (>400 microtubules/field); and nd, not determined. Shaded fields highlight constructs that are particularly efficient in terms of binding affinity, OD_{max}, nucleation, or bundle formation. The correlations show, for example, a high OD_{max} correlates with bundling activity; strong nucleation correlates with strong binding but not necessarily with bundling; and stoichiometries are not correlated with other parameters in an obvious fashion.

the direct binding of τ to microtubules stabilized by taxol; this yields the binding parameters but gives no information about the parameters affecting microtubule growth or dynamics. Light scattering, on the other hand, reflects global nucleation, growth, shrinkage, or bundling, but these parameters are difficult to disentangle. For example, bundling has a disproportionately large effect on light scattering which far outweighs that of growth alone. In order to separate these effects, we have employed video microscopy which yields information on microtubule nucleation and growth separately from bundling.

MATERIALS AND METHODS

Cloning and Expression of Recombinant Constructs of τ Protein. The methods used here were mostly described previously. Briefly, most recombinant human τ proteins were derived from the cDNA clones of Goedert et al. (1988, 1989) and expressed in the pNG2 expression vector, a derivative of

pET-3 (Studier et al., 1990), as described (Biernat et al., 1992). They were prepared using synthetic oligonucleotides for modifying the original τ cDNAs or expression vector sequences by adding or removing restriction enzyme recognition sequences and altering the protein amino acid sequences by cassette mutagenesis (Biernat & Köster, 1987). The cassettes required for replacing or duplicating the sections of the τ cDNA were prepared as synthetic duplex DNA or by polymerase chain reaction (PCR). Alternatively, they were joined independently of restriction enzymes by the method of "splicing by overlap extension" (Horton & Pease, 1991). The human τ isoforms and constructs were expressed in *Escherichia coli* BL21(DE3) strain (Studier et al., 1990). The expressed proteins were purified from bacterial extracts by making use of the heat stability of the protein and by FPLC Mono S (Pharmacia) chromatography. Figure 1 shows a diagram of the domain structure of htau40, the largest isoform in the central nervous tissue (441 residues; all residue numbers refer to this isoform); Table 1 summarizes the structures of the τ constructs. Construct K2 contains residue 1–36 of the bovine τ sequence (Himmler et al., 1989) connected to human τ sequence 243–441 in which the second repeat (residues 275–305) is missing. K6 is a derivative of htau23 without the first repeat (residues 245–274 are missing). K7 is similar to K6 except that the third repeat is missing (residues 306–336). K10 represents the repeat and C-terminal part of htau23 with residues 244–441 (without the second repeat). K12 is similar to K10 but stops at Y394 and contains residues 244–394. K13 is a derivative of htau23 without the first and third repeats (residues 245–336 are missing). K17 contains residues 198–372 without the second repeat (residues 244–274 are missing). K18 represents the 4-repeat domain and contains residues 244–372. K19 is similar to K18 but without the second repeat (residues 244–274 are missing). K23 represents the htau23 molecule without repeats (residues 244–368 are missing). K25 contains the amino terminal domain of htau23 and consists of residues 1–243 (residues 45–102, representing the amino terminal inserts in htau40, are missing). K26 contains residues 369–441. K27 contains residues 198–394 without the second repeat (residues 244–274 are missing). K29 is a htau24 derivative without the third and fourth repeats (residues 306–368 are missing). K30 is a htau24 derivative with the second repeat only (htau24 residues 244–274 and 306–368 are missing). K33 contains residues 198–441 without the second repeat (residues 275–305 are missing). K35 contains residues 151–441 without the second repeat (residues 275–305 are missing). T8R2 contains eight repeats [see Wille et al. (1992)].

Binding Curves. Binding curves between τ and microtubules were measured as described (Gustke et al., 1992). Microtubules were stabilized by taxol which is known not to interfere with the binding of MAPs (Vallee, 1982; Wallis et al., 1993). This allows one to measure binding independently of microtubule assembly or dynamics. The data can be fitted by nonlinear regression using the standard binding equation for a macromolecule containing equivalent and noninteracting ligand binding sites:

$$[\tau_b] = n[Mt_o][\tau_f]/(K_d + [\tau_f])$$

If one plots the bound $[\tau_b]$ vs free $[\tau_f]$ at constant total polymerized ($[Mt_o]$, as in Figure 2), the curve saturates at $\tau_b = n[Mt_o]$, yielding the stoichiometry $n = [\tau_b]/[Mt_o]$. The standard errors in the concentrations ranged from ≈20% (at the lower end, below 1 μM) to ≈3% (in the upper range). The errors in K_d and n are determined from the least-squares fit and are a measure of the internal consistency of the data; they are typically <10% for stoichiometries and 10–20% for dissociation constants. The values quoted in Table 1 are those determined from the nonlinear fit. Note that our procedure differs from that of Butner and Kirschner (1991) or Goode and Feinstein (1994) who titrated a fixed concentration of τ against increasing microtubules. Their 50% saturation point yields an apparent dissociation constant ($K_{d,app}$) since the intrinsic dissociation constant K_d and the stoichiometry n are not determined independently. Hence their $K_{d,app}$ is approximately equivalent to our K_d/n.

Light Scattering. Light scattering was monitored in a Beckman DU 40 spectrophotometer by absorption at 350 nm. The protein (typically 56 μM tubulin dimers mixed with 28 μM τ constructs, corresponding to saturation at $n = 0.5$) was filled into the chamber (depth 1 mm, covered with 50 mm mica windows on both sides) at 4 °C, and the reaction was started by raising the temperature (typically to 37 °C) with defined heating rates (half-time ≈ 4 s). Three parameters were extracted from the curves, the maximum turbidity at steady state, OD_{max}, the maximum rate of assembly, $d(OD)/dt$, and the lag time between the temperature jump and the start of the OD rise.

X-ray Scattering. Experiments were performed on instrument X33 of the EMBL Outstation at the DESY synchrotron laboratory, Hamburg (Koch & Bordas, 1983). Solutions were filled in a 1 mm pathway, thermostated chamber and covered with 50 μm thick mica windows. The cell was connected to a T-jump apparatus (T-jump from 4 to 37 °C, half-time 3–5 s). For data interpretation, see Spann et al. (1987). Briefly, the scattering from dispersed microtubules is characterized by maxima at $S = 0.05$ and 0.09 nm^{-1} (and higher orders; $S = 2 \sin\theta/\lambda$ = Bragg scattering vector). Microtubule bundles generate interparticle interference effects, including peaks with spacings below ≈0.04 nm^{-1}, depending on the packing density.

Video Microscopy. Video microscopy of microtubule nucleation and bundling was done in a similar way as described (Trinczek et al., 1993): 32 μM PC-tubulin and 16 μM τ isoforms or constructs were mixed; 1.0 μL of the samples was put on a slide, covered with 18 × 18 mm coverslips, sealed, and warmed up to 37 °C in a temperature-controlled air flow within 5 s. A constant temperature of 37 °C was maintained by an air flow. Observation was started ≈15 s after a temperature shift to 37 °C; the number of microtubules per volume of the monitor field was recorded by focussing through the whole depth of the field and counted later from the video frames. Ten assembly experiments were done for every construct, and three sequential fields were scored per experiment, within 2 min after the temperature shift and spaced ≈20 s apart (for histograms, see Figure 6). Bundling was assessed from the intensity of the scattered light [in these cases a gray filter ($d = 32$ mm, light passage 25%) was usually necessary in order to avoid saturating the SIT camera]. The monitor field contained an area of 73 × 54 μm^2 (≈4000 μm^2), the depth of the solution was ≈3–4 μm, and the focal depth was ≈1–2 μm.

Miscellaneous. Protein determinations were done by the BCA method (Smith et al., 1985). Electron microscopy of microtubules was done on a Philips CM12 microscope at magnifications around 40000× with 2% uranyl acetate negative staining.

RESULTS

(*a*) *Binding of τ Domains to Microtubules.* A summary of the constructs is given in Table 1. The naturally occurring τ isoforms differ in the number of repeats (R2 may be absent) or inserts (N1, residues 45–73, N2, residues 74–102; one or both may be absent). Synthetic τ molecules were truncated to varying extents on either side of the repeats, and repeats were eliminated, exchanged in position, or duplicated. They were incubated with microtubules stabilized with the drug taxol (Schiff et al., 1979) so that any variation due to microtubule dynamics was eliminated. Bound and free τ were separated by centrifugation and determined as described (Gustke et al., 1992), resulting in binding curves τ_b vs τ_f which yielded dissociation constants and saturation stoichiometries (Figure 2 and Table 1). The curves were interpretable in terms of a single class of equivalent and noninteracting binding sites, consistent with the data of Butner and Kirschner (1991) [this differs from the high molecular weight MAP2 which shows cooperative binding behavior; see Wallis et al. (1993)].

Perhaps the most remarkable feature of the data is that the stoichiometry is highly reproducible, reaching values around $n \approx 0.4$–0.5 with few exceptions (i.e., about 1 τ molecule/2 tubulin dimers or 4 monomers), even for constructs of drastically different sizes. For example, the 3-repeat construct K19 (containing 99 residues) and the largest isoform htau40 (441 residues) bind with similar stoichiometries. To appreciate this, we recall that phosphorylation of a single site (e.g., Ser262) can reduce the stoichiometry 3-fold, down to values around 0.15, lower than that of any of the unphosphorylated constructs in Table 1 (Biernat et al., 1993). The reproducibility of n suggests that the constructs share a common binding motif which covers two dimers on the microtubule surface. The motif could be as small as one or two repeats, plus perhaps some adjacent stretch from domains P or R′. Since whole τ and the repeat domain have highly elongated conformations (>35 and 22 nm, respectively; Wille et al., 1992), one could envisage the τ–microtubule interactions in a variety of ways.

In contrast to the stoichiometry, the dissociation constants K_d vary over a large range, from below 1 μM to above 50 μM (Table 1). Without knowing the 3D-structure of the τ–microtubule interaction, it is obviously difficult to correlate the strength of binding with the sequence, but certain trends emerge from the data of Table 1.

(1) Influence of the projection domain: Cleavage of τ at Tyr197 leaves the assembly domain bound to microtubules and the projection domain free in solution, suggesting that it does not contribute to binding (Steiner et al., 1990). Consistent with this we find that isoforms or constructs that differ only in the projection domain have similar dissociation constants (for example, compare htau40 with htau34 differing in the second insert; htau39 with htau23 differing in both inserts; construct K33 with K35 differing in domain P1). Even if the projection domain is extended to include P2 (construct K25), its binding to microtubules is very weak.

(2) C-terminal tail: As shown for construct K26, the tail by itself binds very weakly, similar to the projection domain. However, when one combines the projection domain and the tail (K23 = K25 + K26), the binding becomes strong, suggesting that the two together act like a "jaw".

(3) Number of repeats: 4-Repeat molecules bind somewhat more tightly than 3-repeat molecules. For example, the K_d value rises ≈3-fold from htau40 to htau39 or ≈2-fold from K18 to K19, but considering the large range of K_d values, this difference appears rather small.

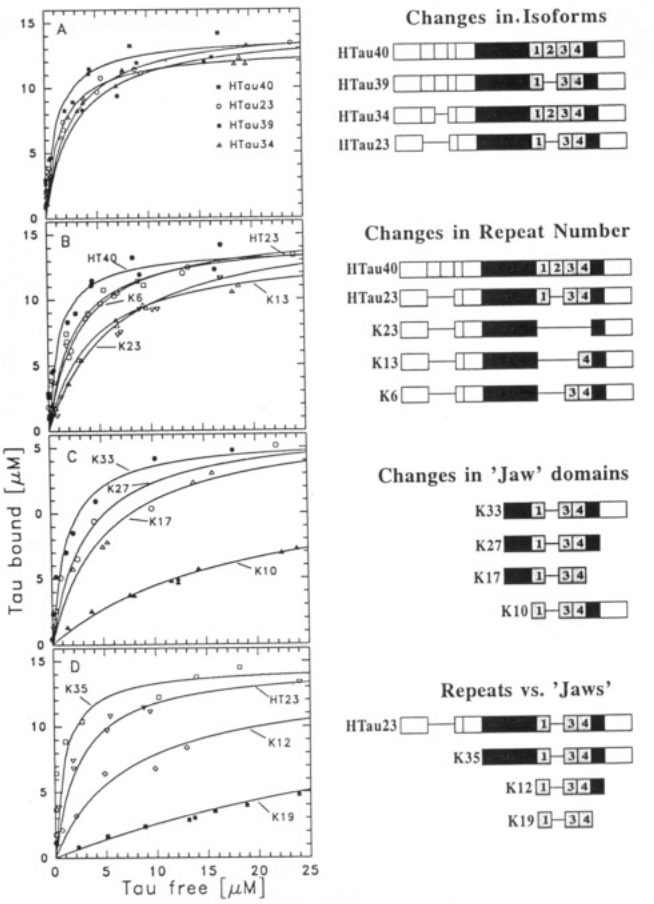

FIGURE 2: Examples of binding curves, plotted as τ_b vs τ_f at 30 μM taxol-stabilized microtubules. The curves were fitted assuming independent binding sites of τ on microtubules, yielding dissociation constants K_d and stoichiometry n at saturation. (A) Four of the six human brain isoforms: htau40 (filled squares), htau39 (filled circles), htau34 (triangles), and htau23 (open circles). The K_d values are in the range 1–3 μM; stoichiometries are 0.43–0.5 τ molecules/tubulin dimer (see Table 1). The curves illustrate that the second repeat R2 strengthens the binding somewhat (K_d decreases about 2-fold) without altering the stoichiometry significantly and that the N-terminal inserts have no influence on binding. (B) τ constructs differing in the number of repeats but having constant flanking regions: four (htau40, filled circles), three (htau23, open squares), two (K6, open circles), one (K13, triangles up), and none (K23, triangles down). The strength of binding decreases with the number of repeats, although not dramatically (K_d increases from ≈1 to ≈6 μM), but there is little variation in the stoichiometry. Note that even the repeatless τ (K23) binds rather well (K_d = 6.5 μM). For comparison, the 8-repeat construct T8R2 binds very tightly in a biphasic manner ($K_{d1} \approx 0.05$ μM, $K_{d2} \approx 10$ μM, not shown, see Table 1). (C) and (D) τ constructs having the same repeat domain (R1-R3-R4, as htau23) but differing in the flanking regions. Constructs containing P2 upstream of the repeats bind rather tightly (e.g., $K_d \approx 5$ μM for K17, triangles in C), and adding the R′ domain improves the binding somewhat (compare K17 and K27, open triangles and circles in (C). Constructs containing just the repeats and C-terminal extensions (K19 and K12 in D, K10 in C) bind more weakly (K_d up to 50 μM for the 3-repeat construct K19); adding the domain R′ strengthens the binding considerably (compare K12), and adding the remaining domain C weakens it again (K10).

(4) Choice and sequence of repeats: Variation of these parameters does not greatly affect the binding. We made a set of 2-repeat τ molecules, derived from htau23 but lacking one repeat, leaving the repeat sequences R1 + R2 (construct K29), R1 + R4 (K7), or R3 + R4 (K6). Notice that all of these constructs contained the R′ domain ("fifth" repeat) and the P domain before repeats. All of these constructs bound tightly; the dissociation constant increased somewhat from 1.2 to 3.1 μM in this series, suggesting again that the type of repeat is of secondary importance. Another set of constructs

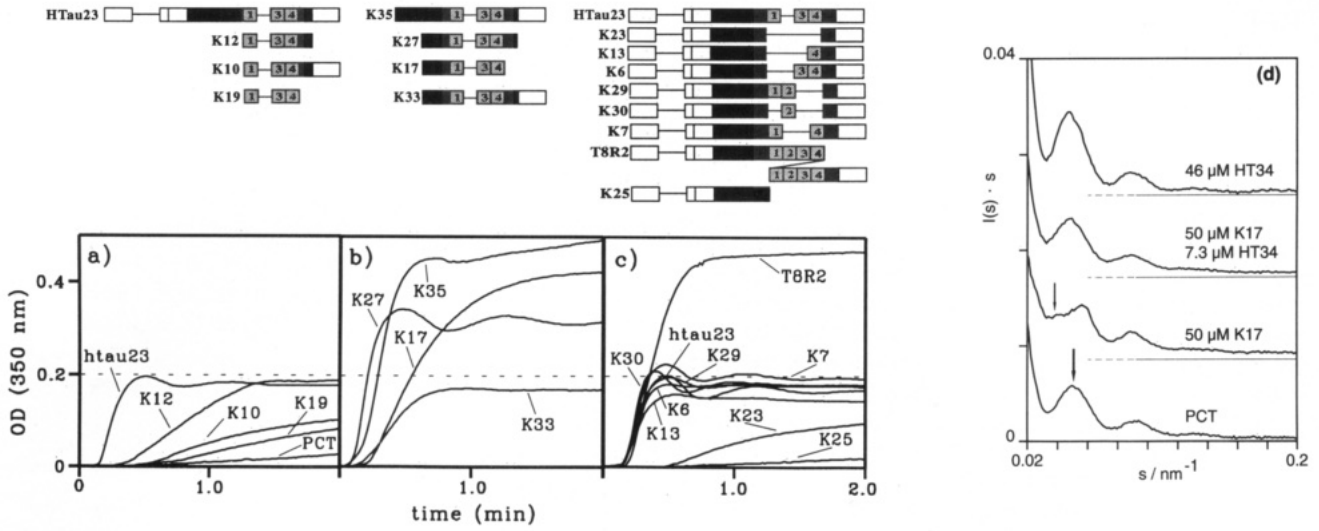

FIGURE 3: Light scattering (a–c) or X-ray scattering (d) of assembling microtubule solutions in the presence of different τ constructs. In the light scattering experiments (a–c), the tubulin concentration was 56 μM, and τ isoforms or constructs were 28 μM. The temperature shift started at time zero. (a) Constructs with three repeats and differing in the C-terminal flanking region of the repeats but without a flanking region on its N-terminal side. Compared with tubulin polymerization without τ, the repeat domain itself (K19) shows a weak assembly-promoting effect. The repeat region plus the short C-terminal flanking sequence R′ (K12) induces pronounced assembly with similar OD_{max} compared to the full-length τ (htau23), but assembly is much slower. Extension of the C-terminus to L441 (K10: R + R′ + C) weakens the effect of R′. (b) Constructs which induce bundle formation as indicated by the increase in OD_{max} compared with the corresponding full-length τ isoform (a, htau23), and as shown below. Constructs including P2 + R (K17), P2 + R + R′(K27), and P1 + P2 + R + R′ + C (K35) increase the final scattering plateau. By contrast, if the whole projection domain is present (htau23, see a) no bundles can be observed. Note that microtubule bundling will additionally increase the scattering signal normally observed for dispersed microtubules in solution. Therefore, it is not possible to directly compare assembly kinetics derived from bundling and not bundling τ constructs. (c) Constructs differing in number and position of single repeats within the repeat domain R keeping N- (N1-N2-P1-P2) and C-terminal (R′-C) flanking regions unchanged. The construct lacking the repeat region (K23) affects assembly only weakly. Introducing only one repeat between the flanking regions (K30: R2; K13: R4) or two repeats (K6: R3 and R4, K7: R1 and R4, K29: R1 and R2) is sufficient to nearly mimic assembly of normal τ (htau23) in these conditions. Furthermore, this behavior is roughly independent of the position and primary sequence of the different repeats R1–R4. In the case of eight repeats embedded in unchanged flanking regions (T8R2), fast assembly and bundling were observed. Neither the N-terminal (K25: N1-N2-P1-P2) nor the C-terminal (K26: R′-C) flanking sequences could promote assembly. (d) X-ray scattering of microtubule solutions assembled from 100 μM tubulin after a temperature jump from 4 to 37 °C in the absence of τ (bottom, PC-tubulin) or in the presence of τ isoform htau34 or construct K17. x-axis: Bragg scattering vector S. y-axis integrated intensity $I(S)\cdot S$ in arbitrary units (displaced vertically for better visibility, as indicated by the base lines on the right). All curves, except the third, show a bell-shaped first maximum near $S = 0.05$ nm^{-1}, typical of dispersed microtubules (large arrow in bottom curve). In the presence of the τ construct K17, interparticle interference becomes visible around 0.038 nm^{-1}, due to the formation of bundles in situ (third curve). This effect does not occur with PC-tubulin (bottom) or with any of the human τ isoforms (e.g., htau34, top), and it is prevented by small amounts of τ isoforms even in the presence of excess K17 (second curve). The experiment shows that certain constructs (e.g., K17) can induce bundling whereas τ isoforms cannot and, in fact, prevent bundling.

contained only one repeat, for example, R2 or R4 (constructs K30 and K13), embedded in the remainder of the htau23 sequence. As before, the binding was tight in both cases. When one eliminates the repeats altogether, leaving only the outside framework of htau23 (as in K23), the construct still binds quite well, with $K_d = 6.5$ μM. This is in stark contrast to the repeats alone whose binding was among the weakest we encountered, with $K_d \approx 25$ μM for 4 repeats, R1 + R2 + R3 + R4 (construct K18), and 50 μM for 3 repeats, R1 + R3 + R4 (K19) (note that single-repeat peptides bind even more weakly, with K_d in the millimolar range; Ennulat et al., 1989; Joly & Purich, 1990).

Summarizing thus far, the repeats by themselves (K18, K19) bind weakly to microtubules. The same is true of the projection domain alone or for the C-terminal tail alone (K25, K26). Clearly, the strong binding to microtubules is not achieved by these domains taken individually.

(5) Combinations of repeats and flanking domains: An explanation for this behavior came from constructs extending from the repeat domain in either direction. For example, if we start from the weakly binding construct K19 (repeats R1 + R3 + R4, $K_d \approx 50$ μM) and add the 25 C-terminal residues (equivalent to most of R′) to form construct K12, it binds 7 times more tightly ($K_d \approx 7$ μM). A similar effect is seen when combining the three repeats of K19 with K26, the whole C-terminal tail, to generate K10 (affinity increases ≈3-fold). In an analogous fashion, we can tighten the binding by combining the repeats with the N-terminal flanking region (for example, K19 + domain P2 = K17, affinity decrease ≈10-fold). By combining the repeats with both flanking regions, the effect is still more pronounced and the binding becomes more than an order of magnitude tighter (K27, $K_d \approx 3$ μM). The improvement in binding is particularly noticeable when the extensions are limited, restricted to, say, P2 or P on the left and/or R′ on the right.

These observations cannot be rationalized by adding up contributions to the binding coming from different domains of τ. Rather, one has to invoke structural constraints which can be met only when certain combinations of domains are in place. Tight binding with K_d in the range below 10 μM is achieved in three conditions: (i) with the repeat region plus the C-terminal extension of R′ (as in K12), (ii) with repeat region plus an N-terminal extension into domain P (as in K17), and (iii) with a combination of C-terminal and N-terminal extensions; in that case, the number and order of intervening repeats is of secondary importance.

(6) Special cases: We mention a few cases that give further insight into the binding behavior. For example, the junctions between the repeat region and the flanking domains must be intact in order to obtain the increased affinity. If R′ is deleted, the binding of τ to microtubules becomes weaker (construct K4, not shown). The same occurs on the N-terminal side if

domain P2 is replaced, say, by domain A (construct K2). Finally, it was mentioned above that increasing the number of repeats improves the binding. This effect can be enhanced by using constructs with duplicated repeat domains, i.e., a total of up to eight repeats (construct T8R2). In these cases, the binding becomes extremely tight ($K_d < 0.5$ μM).

(*b*) *Microtubule Assembly, Nucleation, and Bundling.* τ binds to microtubules, but, more importantly, it alters the assembly characteristics. We therefore asked how the τ constructs affected microtubule assembly and whether the strength of binding correlated with the effects on dynamics. The traditional method of investigating this is light scattering (Gaskin et al., 1974). The parameters deduced from it include the lag time for nucleation (t_{lag}), the initial rate of scattering increase (dOD/dt) which is proportional to the assembly rate (k_+), tubulin concentration (Tu_o), and the microtubule number concentration (MT_o), and the final plateau which is proportional to the total polymer mass (regardless of length distribution). However, this simplified interpretation is valid only within certain boundary conditions; in particular, microtubules need to be homogeneously dispersed. If, instead, they form local inhomogeneities such as bundles, these higher order structures have a strong contribution to the light-scattering signal which mimicks an artificially high degree of assembly. These two effects can be distinguished by other methods, such as X-ray scattering (where the effects of assembly and aggregation are separated into different diffraction angles) or video microscopy where bundling can be observed directly. Another feature detectable by light scattering is that the final plateau is not always steady but often shows fluctuations on the time scale of 1–2 min. These oscillations reflect the synchronized growth and shrinkage of part of the microtubules due to their dynamic instability. Like the lag time, the oscillations are strongly coupled to the nucleation efficiency (Obermann et al., 1990), but since the conditions used here are not optimized for oscillations, we will not discuss them further.

Figure 3 shows light scattering experiments, performed with 56 μM phosphocellulose-purified tubulin (PCT) and different τ constructs (28 μM). The tubulin concentration was chosen such that only marginal assembly occurred over a period of several minutes without τ. If assembly is enhanced by adding τ constructs, the scattering rises rapidly and a plateau is reached usually within 1 min. The lag times, initial slopes, and plateau values are listed in Table 1. Note that the different constructs may promote assembly to the same plateau value (say, about 0.14–0.18 OD in Figure 3a) but with very different lag times and initial slopes (compare htau23 and K12). This means that the extent of assembly and the efficiency of nucleation are distinct features of the process. On the other hand, a short lag time, short half-maximum time, and steep rise in scattering are usually related to one another. The reason is that, in general, a short lag time implies efficient nucleation. This in turn means a high microtubule number concentration, and since this is one of the main factors determining the assembly rate, the half-maximum time is also short [note that MAPs generally affect nucleation much more dramatically than the intrinsic rates of elongation or shortening, as shown by many authors, e.g., Murphy et al. (1977)]. Since Tu_o as well as the Tu_o/τ ratio is constant in our experiments, these factors needs no further considerations. The intrinsic assembly rate k_+ does change with different τ constructs, but this effect is of secondary importance here and will be described in more detail elsewhere.

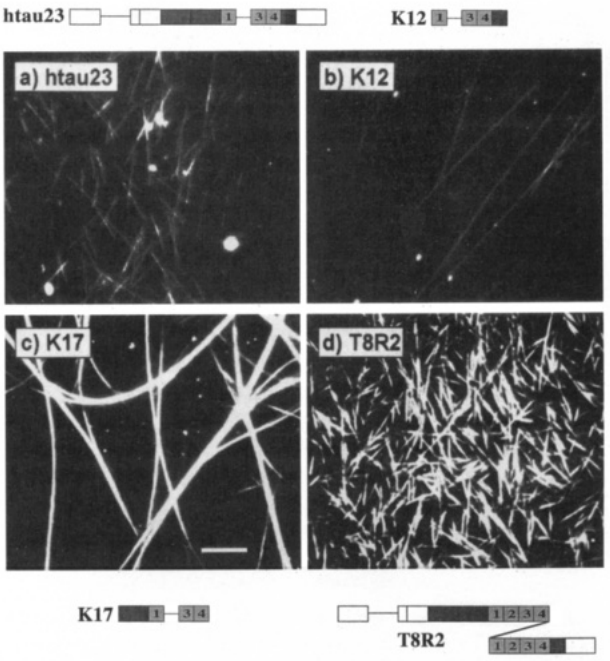

FIGURE 4: Dark field video microscopy of assembling microtubules in tubulin τ preparations. Images showing the whole monitor field (73 × 56 μm^2) were taken around 3 min after the temperature shift. In all cases, tubulin concentration is 32 μM, and that for τ 16 μM. (a) Strong assembly without bundle formation was observed with added htau23. (b) Less microtubules and no bundles were found if K12 was present. (c) Weak assembly combined with bundle formation could be seen with K17. (d) T8R2 induces both strong nucleation and bundles (compare with light scattering curves in Figure 3c). Note that strong nucleation goes with the occurrence of a large number of shorter microtubules (and vice versa), but bundling can occur at both low- and high-number concentrations of microtubules. Images c and d were observed using a grey filter (light passage 25%) to avoid saturation of the SIT camera; bar, 10 μm.

One of the most striking aspects of the scattering curves is that they can be grouped roughly into two categories, one where the plateau is around 0.15–0.20 OD and the other where the plateau is much higher, up to 0.6 OD for the same tubulin concentrations. Since the protein concentrations are similar in the experiments, this cannot explain the difference. Electron microscopy (Figure 5) and X-ray scattering (Figure 3d) confirm that the assembly products are microtubules and not some other polymorphic structures. The explanation for the high light scattering is that the microtubules are not nucleated homogeneously throughout the solution but rather in local clusters which stay together as bundles during growth. These higher order structures cause a strong additional contribution to the turbidity (similar to scattering from colloids).

The distinction between dispersed and bundled microtubules becomes evident in the X-ray experiments because they are sensitive to interparticle interference effects. Homogeneously dispersed microtubules show a first subsidiary maximum around 0.05 nm^{-1} which arises from the diameter of the microtubule cylinder [e.g., Figure 3d, top or bottom; for details, see Spann et al. (1987)]. Gels of homogeneously bundled microtubules show several changes, for example, an additional interparticle interference peak around 0.038 nm^{-1} (depending on the mean spacing). Solutions with partially bundled microtubules show intermediate patterns, such as in Figure 3d, curve 3.

The effect of different τ constructs on microtubule assembly and bundling can be seen directly by dark field video microscopy. We had observed earlier that bundling becomes prominent in the conditions of microtubule oscillations where

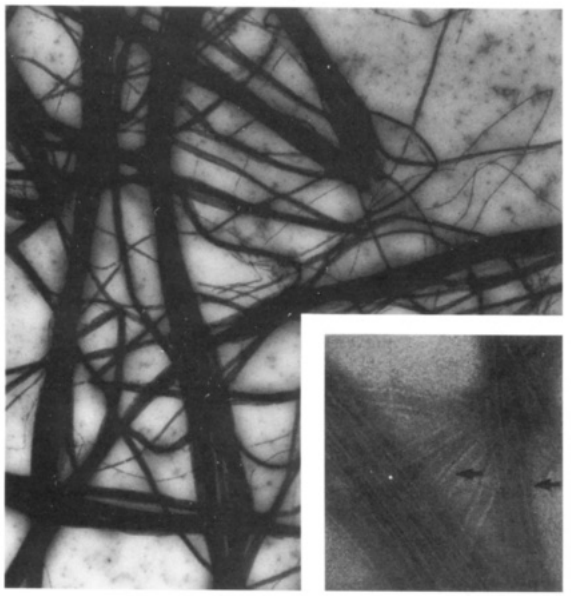

FIGURE 5: Electron microscopy of microtubule bundles induced by construct K17. Tubulin (30 μM) and 15 μM K17 were polymerized for 10 min at 37 °C and then diluted 3-fold, placed on a carbon-coated grid, and negatively stained (2% uranyl acetate). Note that microtubule walls almost touch each other in these bundles (arrows). Magnification: ×26000; insert, ×310000.

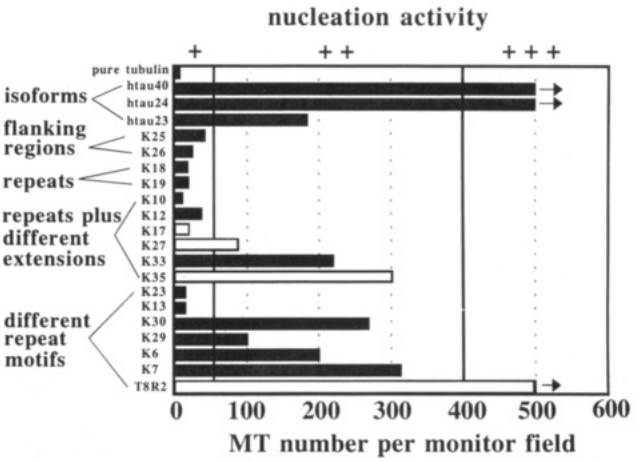

FIGURE 6: Histogram showing microtubule nucleation in the presence of different τ constructs (for experimental procedure and data collection, see the methods). We separate the nucleation activity into three categories: weak (+), <50 microtubules/field; medium (+ +), 100–400 microtubules/field; and strong (+ + +), ≫400 microtubules/field. This crude classification was chosen since the number of microtubules per field varied over a wide range, reflecting the inhomogeneities within each sample. By contrast, in the case of strongly nucleating preparations (+ + +), the reaction started homogeneously ≈15 s after the temperature shift. In these cases, the number of microtubules tends to be underestimated because of their overlap (thus a lower limit of 500 microtubules/field is shown for htau40, htau24, and T8R2, arrows). Empty bars show τ constructs which induce microtubule bundles (see Figures 3 and 4).

the nucleation and decay of microtubules are self-synchronized (Mandelkow et al., 1989). Although closely juxtaposed microtubules are generally not resolved by the technique, bundle formation can be detected because the contrast is strongly enhanced (Figure 4). Because the field of view is limited (≈4000 μm^2), quantitation can only be approximate. However, the distinction between strong or poor nucleation, or between single microtubules and microtubule bundles, is quite striking and unambiguous.

This was verified by electron microscopy (Figure 5); τ constructs that induced high OD in light scattering or microtubule bundles in video microscopy showed them in electron microscopy as well. The packing of these bundles was remarkably tight, i.e., microtubule walls often appeared to be touching each other with very little space in between. Moreover, the bundles were stable enough to survive the preparation for negative staining. A comparison of the nucleation and bundling efficiencies of different constructs is given in Figure 6, based on the number of dispersed microtubules and bundles observed by video microscopy.

What constructs cause efficient nucleation or bundling? Firstly, we note that none of the τ isoforms (htau23 ... htau40) induce bundling, even though they bind tightly, have the usual stoichiometry ($n \approx 0.5$), and nucleate efficiently. This emphasizes that bundling and nucleation are distinct features of τ. In fact, the majority of constructs we have tested, including both poor and efficient nucleators, do not induce bundling. Constructs that comprise of only the repeats are poor nucleators; they do not cause bundling either. Both would be consistent with their weak affinity for microtubules. Thus, the bundling capacity must reside in combinations of domains larger than the repeats but smaller than whole τ. Among the constructs tested so far, there is good correlation between bundling and a combination of repeats plus the proline-rich domain (P or just P2, upstream of the repeats). This is illustrated by constructs such as K17, K27, and K35. Addition of the N-terminal domains A + B abrogates the bundling (as in the τ isoforms or in constructs such as K6 and K29, etc). The exception to this rule is the construct T8R2 where the duplication of the repeat domain appears to overcome the inhibition by the N-terminal domains in terms of bundling capacity. Similarly, addition of the C-terminal tail C reduces bundling (compare K17 with K33), although this inhibition can be overcome by adding more of the P domain (compare K33 with K35). These results can be explained by the charge distribution of τ. The domains P, R, and R′ are basic, they compensate the negative charge of microtubules and thus allow them to approach each other. Domains A and C are acidic and thus add to the repulsion between microtubules, i.e., these domains can be regarded as spacer domains.

These experiments allow several conclusions. (i) Microtubules can indeed be bundled by certain τ constructs, but this requires nucleation in the presence of the constructs. (ii) None of the native τ isoforms are bundlers; instead they inhibit bundle formation and must rather be considered as spacers.

DISCUSSION

τ is a neuron-specific microtubule-associated protein which appears to be necessary for the formation and stabilization of axons (Baas et al., 1991). In the pathological conditions of Alzheimer's disease, τ aggregates independently of microtubules, forming the paired helical filaments of the neurofibrillary tangles [for reviews, see Kosik (1992) and Lee and Trojanowski (1992)]. These findings have recently generated much interest in the cell biology function of τ. Following the cloning of τ and the elucidation of its gene structure (Drubin et al., 1984; Lee et al., 1988; Goedert et al., 1988; Himmler et al., 1989; Andreadis et al., 1992), it became possible to investigate the relationship between τ structure and function in a systematic fashion. Of immediate interest was the domain containing the three or four repeats. Several authors showed that they supported microtubule binding (Aizawa et al., 1989; Lee et al., 1989; Ennulat et al., 1989; Joly & Purich, 1990; Butner & Kirschner, 1991; Goode & Feinstein, 1994), but there was the curious discrepancy that the repeats alone bound rather weakly, with K_d in the

millimolar range. The second region of obvious interest was the two near N-terminal inserts. This region does not bind to microtubules, and thus no clear-cut function has emerged so far, although the recent discovery of "big τ" in the peripheral nervous system (Couchie et al., 1992) with more inserts in the N-terminal domain suggests some cell-specific and perhaps developmentally regulated function.

In this report we have attempted to dissect the functions of τ domains with respect to microtubule behavior. We have synthesized a large number of τ constructs in *E. coli* and probed their interactions with microtubules using several techniques. Before discussing the results, it may be useful to recall what properties of microtubules one would like to understand. Neuronal microtubules are dynamically unstable (Mitchison & Kirschner, 1984), they must be nucleated, they grow, and they shrink. This can be described by molecular association rates, dissociation rates, and transition frequencies from growth to shrinkage ("catastrophe"; Walker et al., 1988) and vice versa ("rescue"). Since there are no obvious microtubule nucleation sites in axons (Baas & Joshi, 1992), dynamics could happen both at the plus and minus ends, thus doubling the number of rate constants to be determined. In principle, τ or other MAPs (e.g., STOP proteins; Margolis et al., 1990) could regulate the dynamics; in practice, τ appears to affect only a subset of the rate constants (Drechsel et al., 1992). In addition, there might be other functions of τ. Cells transfected with τ form microtubules arrayed in parallel bundles (Kanai et al., 1989, 1992; Knops et al., 1991), and the spacing between microtubules depends on the size of the projection domain (Chen et al., 1992). Neuronal microtubules provide the tracks for axonal transport by motor proteins such as kinesin or dynein [for review, see Walker & Sheetz (1993)], and it is conceivable that this is affected by τ. Finally, τ and other MAPs could act as an anchor for other proteins or enzymes, as suggested by the binding of PKA to MAP2 (Obar et al., 1989) or of MAP kinase and GSK-3 to MAPs (Mandelkow et al., 1992). The "classical" function of τ is to stabilize microtubules (Cleveland et al., 1977; Drubin & Kirschner, 1986), but this and the other possible functions of τ need not be coupled to one another, and therefore it is necessary to assay them separately. The approximate assignment of τ domains to different functions is depicted in Figure 7, top.

In order to understand τ's function, we also recall some properties of τ determined previously. τ is a highly elongated structure with almost no detectable secondary structure (Cleveland et al., 1977). In the electron microscope, it appears as a rod of lengths around 35 nm (≈22 nm for the repeat domain alone); it is capable of associating into antiparallel dimers of roughly the same length, and the repeat domain can self-assemble into paired helical filaments similar to those of Alzheimer's disease (Wille et al., 1992). The lengths of τ constructs set important constraints on the types of interactions between τ and the microtubule lattice. This becomes obvious when one considers stoichiometries of binding: Microtubules can be saturated at a ratio of 1 τ/2 tubulin dimers ($n = 0.5$), but upon phosphorylation, this value drops to 1 τ/6 dimers ($n \approx 0.16$), equivalent to a length along a protofilament of 6 × 8 = 48 nm (Gustke et al., 1992; Biernat et al., 1993). These numbers immediately suggest that τ in solution must differ in major ways from τ bound to a microtubule.

In our present study, we have addressed part of the questions mentioned above. We have studied the binding of τ constructs to microtubules in conditions where microtubule dynamics is eliminated by taxol. We have looked for the capacity of τ

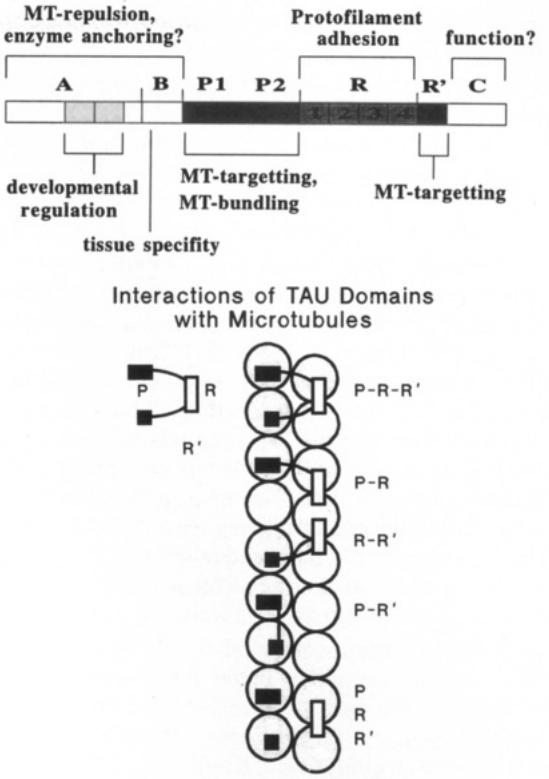

FIGURE 7: Roles of τ domains. (top) Domains of τ with probable functional assignment. Domains A and B have the effect of keeping macromolecules spaced apart; the inserts in A (gray) are developmentally regulated (Goedert et al., 1989); another insert in B (not shown) distinguishes peripheral nerve τ ("big tau", Couchie et al., 1992) from central nerve τ. Domains P supports microtubule binding and bundling, repeats R make the binding productive in terms of assembly, R′ aids in binding, and the function of C is not known. (bottom) Diagram illustrating the "jaws" effect and the difference between productive and unproductive binding. The domains P, R, and R′ are simplified as boxes. The "jaws" P and R′ are black, and P is drawn larger than R′ to emphasize that it promotes binding of τ better. A construct which not only binds to microtubules but also strongly stimulates assembly (in terms of short lag time, high initial rate, and/or high final OD, see Table 1) is considered to bind productively. Such a construct is depicted to bind across protofilaments to emphasize that it promotes cohesion between protofilaments. Other constructs do not promote assembly, or only weakly, and are thus considered to bind less productively or unproductively (such as K23, the two jaws without repeats). Thus, combinations P-R-R′ (e.g., htau40) and P-R (e.g., K17) bind strongly and productively; combination R-R′ (e.g., K10, K12) binds more weakly and less productively; combination P-R′ (K23) binds rather strongly but unproductively, and each of the domains P, R, and R′ (K25, K18, K26) alone binds weakly and unproductively. The domains A, B, and C are not shown for simplicity. Note that the diagrams are idealized oversimplifications because the structure of bound τ is not known.

constructs to initiate microtubule assembly (nucleation and elongation) and for the formation of microtubule bundles. The effects of τ constructs on rate constants of assembly and disassembly, the transition frequencies between growth and shrinkage, and the effects of phosphorylation will be dealt with elsewhere.

The binding of τ to taxol-stabilized microtubules can be summarized as follows: Constructs that bind to any measurable extent do so with similar stoichiometries, around $n \approx 0.5$ (1 τ/2 dimers). This is perhaps the most remarkable result, especially since it holds both for strongly binding and weakly binding constructs. Its simplest interpretation is that two tubulin dimers must be involved to get appreciable binding of τ. The reproducibility of the binding must be seen in the context of phosphorylation of Ser262 where the stoichiometry

drops 3-fold (as if six dimers were needed for binding), again almost independently of the strength of binding.

In contrast to the stoichiometry, the apparent dissociation constants K_d vary considerably, from 1 μM and less to 50 μM and more. In the absence of 3D-structure information, it may seem somewhat daring to correlate the K_d values with the domain composition of τ, but some principles have emerged. They include the following (see Figure 1 and Table 1).

(i) Like other MAPs such as MAP2 (Vallee, 1980), τ can be cleaved by chymotrypsin into two major domains at Tyr197 (Steiner et al., 1990). The projection domain is N-terminal (Met1–Tyr197, Proj = A + B + P1), and it does not bind measurably to microtubules; the C-terminal assembly domain (Ser198–Leu441, Ass = P2 + R + R′ + C) binds strongly (K_d in the micromolar range). As a corollary, the number of N-terminal inserts in A has no influence on the binding. Thus, alternative splicing in the N-terminal region probably has a role other than microtubule binding. These could include the spacing between microtubules and other structures [cf. Chen et al., 1992)] or the anchoring of other proteins (analogous to PKA in MAP2; Obar et al., 1989).

(ii) Native τ isoforms all bind tightly ($K_d \approx 1$–3 μM), 4-repeat isoforms somewhat better than 3-repeat isoforms. Thus, although the number of repeats and inserts is developmentally regulated (three repeats, no inserts in fetal tissue and all isoforms in adult tissue; Kosik et al., 1989), the small difference in binding would suggest that this is unlikely to be the reason for alternative splicing. One should note, however, that a few residues in the linker region between R1 and R2 play a special role in the binding of τ to microtubules (Goode & Feinstein, 1994).

(iii) The repeat domain alone binds poorly ($K_d \approx 25$–50 μM). This is in agreement with earlier studies on peptides derived from the repeat region; one repeat alone binds even more weakly, with K_d in the millimolar range (Ennulat et al., 1989; Joly et al., 1990). Because of this, one might even question whether the repeats deserve to be called a microtubule-binding domain. By contrast, a τ construct that lacks the repeats (K23) binds quite well, although it is a weak nucleator. Since even K23 induces apparently normal microtubules, this means that the repeats are not crucial for the formation of the microtubule lattice. Finally, the parts to the left and right of the repeats show negligible binding by themselves (K25, K26). The simplest interpretation of these data is that one needs a sufficiently large combination of the domains P, R, and R′ to obtain tight binding, and that the flanking regions (P and R′) contribute substantially to the binding, forming "jaws" as it were (Figure 7). Within the repeats, the data of Butner and Kirschner (1991) showed that the binding capacity was broadly distributed, with a recent refinement by Goode and Feinstein (1994) who demonstrated an enhancing effect in the linker region between R1 and R2. Our data add to this interpretation the importance of the flanking regions, at least one of which was present in most constructs used by the other groups and therefore explains the relatively strong binding they found. A special enhancement of binding through the second repeat can be inferred by comparing single-repeat constructs flanked by both jaws, such as K13 and K30 (Table 1).

One could even think of a more subtle interpretation: We have shown elsewhere that τ can form antiparallel dimers and hairpin-like structures (Wille et al., 1992). In addition, the reactivities of certain antibodies suggest that sequences on both sides of the repeats come together to form an epitope (e.g., antibody SMI34; Lichtenberg et al., 1992). This could mean that strong binding and nucleation depend on a conformation which is optimized only when regions P and R′ cooperate across the repeats. Interestingly, τ can be phosphorylated by MAP kinase at Ser–Pro motifs, most of which are located in domains P and R′; this phosphorylation transforms τ into an "Alzheimer-like" state as judged by antibodies (such as SMI34 and others) which discriminate between normal τ and τ from paired helical filaments (Drewes et al., 1992; Biernat et al., 1992). These observations suggest that particular conformations of τ would be important not only for binding to microtubules but also for aggregation into paired helical filaments.

Microtubule Bundling and Cross-Linking. The question of microtubule bundling by τ and other MAPs has received much attention in recent years. They were triggered in particular by the observation that transfection or microinjection of cells with τ or MAP2 induced the formation of parallel arrays of microtubules (Kanai et al., 1989; Lewis et al., 1989; Knops et al., 1991; Lee & Rook, 1992; Chen et al., 1992; Weisshaar et al., 1992). This suggested a mechanism of neurite outgrowth via cross-linked microtubule bundles. On the other hand, our results show clearly that τ isoforms do not cross-link microtubules; they are both strong nucleators and strong spacers, i.e., they keep microtubules apart. The spacer function resides mainly in the N-terminal domains A and B; once they are deleted, combinations of the domains P, R, or R′ can induce tight bundling. Similar observations were reported by others [e.g., Brandt and Lee (1993) for τ; Aizawa et al. 1991) for MAP4], and the spacer functions of the N-terminal domains were emphasized by Chen et al. (1992) who compared τ, MAP2c, and MAP2.

Can this apparent contradiction be resolved? In our view, the terms "bundle" and "cross-link" need to be defined more precisely. A bundle is an array of parallel filaments, irrespective of how it was generated. Cross-links are elements that tie the filaments together. For instance, actin filaments can be cross-linked by actin-binding proteins, which have two F-actin binding sites (as monomers or dimers) and thus link two actin filaments firmly at a specified distance; here the cross-linking and spacing functions are combined in the same structure [for example, Noegel et al. (1989)]. This does not happen with any of the τ isoforms in the case of microtubules, and thus τ cannot be considered a cross-linker.

How, then, could microtubule bundles be generated in cells or in solution? The simplest answer is that when many microtubules are nucleated in a restricted area and stabilized by τ or its derivatives, they will form parallel arrays, i.e., bundles. The distance between the microtubules will be determined by their local density, but it will not be less than the size of the projection domain of τ (because of the spacer function). Such oriented bundles can be formed in vitro if the nucleation is sufficiently enhanced by certain τ constructs. To get parallel microtubules, it is not even necessary to have τ as a spacer; the repulsive force of the negatively charged cylinders acts as a spacer in itself [for the case of F-actin, see Matsudaira et al. (1983)]. Nor are special microtubule-organizing structures necessary; in fact, Weisshaar et al. (1992) showed that a strong nucleator can override the MTOC of a cell to generate microtubule bundles independently of the MTOC. In summary, the above considerations suggest a way by which τ (or other MAPs) could generate bundles of microtubules without being cross-linking proteins themselves.

ACKNOWLEDGMENT

We thank U. Böning and N. Burmester for excellent technical assistance, A. Marx and M. Kniel for help with the

light and X-ray scattering experiments, M. Goedert (MRC Cambridge) for generously providing the human τ cDNA clones, and M. Koch (EMBL) for making the X-ray instrument X33 available.

REFERENCES

Aizawa, H., Kawasaki, H., Murofushi, H., Kotani, S., Suzuki, K., & Sakai, H. (1989) *J. Biol. Chem. 264*, 5885–5890.

Aizawa, H., Emori, Y., Murofushi, H., Kawasaki, H., & Suzuki, K. (1990) *J. Biol. Chem. 265*, 13849–13855.

Aizawa, H., Emori, Y., Mori, A., Murofushi, H., Sakai, H., & Suzuki, K. (1991) *J. Biol. Chem. 266*, 9841–9846.

Andreadis, A., Brown, W. M., & Kosik, K. S. (1992) *Biochemistry 31*, 10626–10633.

Baas, P. W., & Joshi, H. C. (1992) *J. Cell Biol. 119*, 171–178.

Baas, P. W., Pienkowski, T. P., & Kosik, K. S. (1991) *J. Cell Biol. 115*, 1333–1344.

Baumann, K., Mandelkow, E.-M., Biernat, J., Piwnica-Worms, H., & Mandelkow, E. (1993) *FEBS Lett. 336*, 417–424.

Biernat, J., & Köster, H. (1987) *Protein Eng. 1*, 353–358.

Biernat, J., Mandelkow, E.-M., Schröter, C., Lichtenberg-Kraag, B., Steiner, B., Berling, B., Meyer, H. E., Mercken, M., Vandermeeren, A., Goedert, M., & Mandelkow, E. (1992) *EMBO J. 11*, 1593–1597.

Biernat, J., Gustke, N., Drewes, G., Mandelkow, E.-M. & Mandelkow, E. (1993) *Neuron 11*, 153–163.

Bramblett, G. T., Goedert, M., Jakes, R., Merrick, S. E., Trojanowski, J. Q., & Lee, V. M. Y. (1993) *Neuron 10*, 1089–1099.

Brandt, R., & Lee, G. (1993) *J. Biol. Chem. 268*, 3414–3419.

Brugg, B., & Matus, A. (1991) *J. Cell Biol. 114*, 735–743.

Butner, K. A., & Kirschner, M. W. (1991) *J. Cell Biol. 115*, 717–730.

Chapin, S. J., & Bulinski, J. C. (1991) *J. Cell Sci. 98*, 27–36.

Chapin, S. J., & Bulinski, J. C. (1992) *Cell Motil.-Cytoskeleton 23*, 236–243.

Chen, J., Kanai, Y., Cowan, N., & Hirokawa, N. (1992) *Nature 360*, 674–677.

Cleveland, D. W., Hwo, S.-Y., & Kirschner, M. W. (1977) *J. Mol. Biol. 116*, 207–225.

Couchie, D., Mavilia, C., Georgieff, I., Liem, R., Shelanski, M., & Nunez, J. (1992) *Proc. Natl. Acad. Sci. U.S.A. 89*, 4378–4381.

Drechsel, D. N., Hyman, A. A., Cobb, M. H., & Kirschner, M. W. (1992) *Mol. Biol. Cell 3*, 1141–1154.

Drewes, G., Lichtenberg-Kraag, B., Döring, F., Mandelkow, E.-M., Biernat, J., Goris, J., Doree, M., & Mandelkow, E. (1992) *EMBO J. 11*, 2131–2138.

Drubin, D., & Kirschner, M. (1986) *J. Cell Biol. 103*, 2739–2746.

Drubin, D., Caput, D. & Kirschner, M. (1984) *J. Cell Biol. 98*, 1090–1097.

Ennulat, D. J., Liem, R. K. H., Hashim, G. A., & Shelanski, M. L. (1989) *J. Biol. Chem. 264*, 5327–5330.

Erickson, H. P., & Voter, W. A. (1976) *Proc. Natl. Acad. Sci. U.S.A. 73*, 2813–2817.

Gaskin, F., Cantor, C. R., & Shelanski, M. L. (1974) *J. Mol. Biol. 89*, 737–758.

Goedert, M., & Jakes, R. (1990) *EMBO J. 9*, 4225–4230.

Goedert, M., Wischik, C., Crowther, R., Walker, J., & Klug, A (1988) *Proc. Natl. Acad. Sci. U.S.A. 85*, 4051–4055.

Goedert, M., Spillantini, M., Jakes, R., Rutherford, D., & Crowther, R. A. (1989) *Neuron 3*, 519–526.

Goode, B. L., & Feinstein, S. C. (1994) *J. Cell Biol. 124*, 769–782.

Grundke-Iqbal, I., Iqbal, K., Tung, Y., Quinlan, M., Wisniewski, H., & Binder, L. (1986) *Proc. Natl. Acad. Sci. U.S.A. 83*, 4913–4917.

Gustke, N., Steiner, B., Mandelkow, E.-M., Biernat, J., Meyer, H. E., Goedert, M., & Mandelkow, E. (1992) *FEBS Lett. 307*, 199–205.

Himmler, A., Drechsel, D., Kirschner, M., & Martin, D. (1989) *Mol. Cell. Biol. 9*, 1381–1388.

Horton, R. M., & Pease, L. R. (1991) in *Directed Mutagenesis, A Practical Approach* (McPherson, M. J., Ed.) pp 217–247, IRL Press, Oxford.

Ishiguro, K., Omori, A., Sato, K., Tomizawa, K., Imahori, K., & Uchida, T. (1991) *Neurosci. Lett. 128*, 195–198.

Joly, J. C., & Purich, D. L. (1990) *Biochemistry 29*, 8916–8920.

Kanai, Y., Takemura, R., Oshima, T., Mori, H., Ihara, Y., Yanagisawa, M., Masaki, T., & Hirokawa, N. (1989) *J. Cell Biol. 109*, 1173–1184.

Kanai, Y., Chen, J., & Hirokawa, N. (1992) *EMBO J. 11*, 3953–3961.

Kindler, S., Schulz, B., Goedert, M., & Garner, C. C. (1990) *J. Biol. Chem. 265*, 19679–19684.

Knops, J., Kosik, K., Lee, G., Pardee, J., Cohengould, L., & McConlogue, L. (1991) *J. Cell Biol. 114*, 725–733.

Koch, M. H. J., & Bordas, J. (1983) *Nucl. Instrum. Methods 208*, 461–469.

Kosik, K. S. (1992) *Science 256*, 780–783.

Kosik, K. S., Orecchio, Bakalis, S., & Neve, R. L. (1989) *Neuron 2*, 1389–1397.

Lee, G. (1993) *Curr. Opin. Cell Biol. 5*, 88–94.

Lee, G., & Rook, S. (1992) *J. Cell. Sci. 102*, 227–237.

Lee, G., Cowan, N., & Kirschner, M. (1988) *Science 239*, 285–288.

Lee, G., Neve, R. L., & Kosik, K. S. (1989) *Neuron 2*, 1615–1624.

Lee, V. M. Y., & Trojanowski, J. Q. (1992) *Curr. Opin. Neurobiol. 2*, 653–656.

Lewis, S. A., Wang, D., & Cowan, N. J. (1988) *Science 242*, 936–939.

Lewis, S. A., Ivanov, I. E., Lee, G. H., & Cowan, N. J. (1989) *Nature (London) 342*, 498–505.

Lichtenberg-Kraag, B., Mandelkow, E.-M., Biernat, J., Steiner, B., Schröter, C., Gustke, N., Meyer, H. E., & Mandelkow, E. (1992) *Proc. Natl. Acad. Sci. U.S.A. 89*, 5384–5388.

Mandelkow, E., Mandelkow, E.-M., Hotani, H., Hess, B., & Müller, S. C. (1989) *Science 246*, 1291–1293.

Mandelkow, E. M., Drewes, G., Biernat, J., Gustke, N., Van Lint, J., Vandenheede, J. R., & Mandelkow, E. (1992) *FEBS Lett. 314*, 315–321.

Margolis, R. L., Rauch, C. T., Pirollet, F., & Job, D. (1990) *EMBO J. 9*, 4095–4102.

Matsudaira, P., Mandelkow, E., Renner, W., Hesterberg, L., & Weber, K. (1983) *Nature (London) 301*, 209–214.

Mitchison, T., & Kirschner, M. (1984) *Nature (London) 312*, 237–242.

Noegel, A., Rapp, S., Lottspeich, F., Schleicher, M., & Stewart, M. (1989) *J. Cell Biol. 109*, 607–618.

Obar, R. A., Dingus, J., Bayley, H., & Vallee, R. B. (1989) *Neuron 3*, 639–645.

Obermann, H., Mandelkow, E.-M., Lange, G., & Mandelkow, E. (1990) *J. Biol. Chem. 265*, 4382–4388.

Schiff, P. B., Fant, J., & Horwitz, S. B. (1979) *Nature (London) 277*, 665–667.

Schulz, G. E., & Schirmer, R. H. (1979) *Principles of Protein Structure*, Springer Verlag, Heidelberg.

Smith, P., Krohn, I., Hermanson, G., Mallia, A., Gartner, F., Provenzano, M., Fujimoto, E., Goeke, N., Olson, B., & Klenk, D. (1985) *Anal. Biochem. 150*, 76–85.

Spann, U., Renner, W., Mandelkow, E.-M., Bordas, J., & Mandelkow, E. (1987) *Biochemistry 26*, 1123–1132.

Steiner, B., Mandelkow, E.-M., Biernat, J., Gustke, N., Meyer, H. E., Scmidt, B., Mieskes, G., Söling, H. D., Drechsel, D., Kirschner, M. W., Goedert, M., & Mandelkow, E. (1990) *EMBO J. 9*, 3539–3544.

Studier, W. F., Rosenberg, A. H., Dunn, J. J., & Dubendorff, J. W. (1990) *Methods Enzymol. 185*, 60–89.

Trinczek, B., Marx, A., Mandelkow, E.-M., Murphy, D. B., & Mandelkow, E. (1993) *Mol. Biol. Cell 4*, 323–335.

Vallee, R. B. (1980) *Proc. Natl. Acad. Sci. U.S.A. 77*, 3206–3210.
Vallee, R. B. (1982) *J. Cell Biol. 92*, 435–442.
Vallee, R. B., & Borisy, G. G. (1977) *J. Biol. Chem. 252*, 377–382.
Walker, R., & Sheetz, M. P. (1993) *Annu. Rev. Biochem. 62*, 429–451.
Walker, R., O'Brien, E., Pryer, N., Soboeiro, M., Voter, W., Erickson, H., & Salmon, E. (1988) *J. Cell Biol. 107*, 1437–1448.
Wallis, K., Azhar, S., Rho, M., Lewis, S., Cowan, N., & Murphy, D. B. (1993) *J. Biol. Chem. 268*, 15158–15167.
Weingarten, M. D., Suter, M. M., Littman, D. R., & Kirschner, M. W. (1974) *Biochemistry 13*, 5529–5537.
Weisshaar, B., Doll, T., & Matus, A. (1992) *Development 116*, 1151–1161.
West, R. R., Tenbarge, K. M., & Olmsted, J. B. (1991) *J. Biol. Chem. 266*, 21886–21896.
Wiche, G., Oberkanins, C., & Himmler, A. (1991) *Int. Rev. Cytol. 124*, 217–273.
Wille, H., Drewes, G., Biernat, J., Mandelkow, E.-M., & Mandelkow, E. (1992) *J. Cell Biol. 118*, 573–584.
Wischik, C., Novak, M., Thogersen, H., Edwards, P., Runswick, M., Jakes, R., Walker, J., Milstein, C., Roth, M., & Klug, A. (1988) *Proc. Natl. Acad. Sci. U.S.A. 85*, 4506–4510.
Wood, J., Mirra, S., Pollock, N., & Binder, L. (1986) *Proc. Natl. Acad. Sci. U.S.A. 83*, 4040–4043.